Return Period of Soil Liquefaction

Steven L. Kramer, M.ASCE[1]; and Roy T. Mayfield[2]

Abstract: The paper describes a performance-based approach to the evaluation of liquefaction potential, and shows how it can be used to account for the entire range of potential ground shaking. The result is a direct estimate of the return period of liquefaction, rather than a factor of safety or probability of liquefaction conditional upon ground shaking with some specified return period. As such, the performance-based approach can be considered to produce a more complete and consistent indication of the actual likelihood of liquefaction at a given location than conventional procedures. In this paper, the performance-based procedure is introduced and used to compare likelihoods of the initiation of liquefaction at identical sites located in areas of different seismicity. The results indicate that the likelihood of liquefaction depends on the position and slope of the peak acceleration hazard curve, and on the distribution of earthquake magnitudes contributing to the ground motion hazard. The results also show that the consistent use of conventional procedures for the evaluation of liquefaction potential produces inconsistent actual likelihoods of liquefaction.

DOI: 10.1061/(ASCE)1090-0241(2007)133:7(802)

CE Database subject headings: Earthquakes; Liquefaction; Sand; Penetration tests; Hazards.

Introduction

Liquefaction of soil has been a topic of considerable interest to geotechnical engineers since its devastating effects were widely observed following 1964 earthquakes in Niigata, Japan and Alaska. Since that time, a great deal of research on soil liquefaction has been completed in many countries that are exposed to this important seismic hazard. This work has resulted in the development of useful empirical procedures that allow the deterministic and probabilistic evaluation of liquefaction potential for a specified level of ground shaking.

In practice, the level of ground shaking is usually obtained from the results of a probabilistic seismic hazard analysis (PSHA); although that ground shaking model is determined probabilistically, a single level of ground shaking is selected and used within the liquefaction potential evaluation. In reality, though, a given site may be subjected to a wide range of ground shaking levels ranging from low levels that occur relatively frequently to very high levels that occur only rarely, each with different potential for triggering liquefaction.

This paper shows how the entire range of potential ground shaking can be considered in a fully probabilistic liquefaction potential evaluation using a performance-based earthquake engineering (PBEE) framework. The result is a direct estimate of the return period of liquefaction, rather than a factor of safety or probability of liquefaction conditional upon ground shaking with some specified return period. As such, the performance-based approach can be considered to produce a more complete and consistent indication of the likelihood of liquefaction at a given location than conventional procedures. In this paper, the performance-based procedure is introduced and then used to compare the actual likelihoods of liquefaction at identical sites located in areas of different seismicity; the results show that the consistent use of conventional procedures for evaluation of liquefaction potential produces inconsistent actual likelihoods of liquefaction.

Liquefaction Potential

Liquefaction potential is generally evaluated by comparing consistent measures of earthquake loading and liquefaction resistance. It has become common to base the comparison on cyclic shear stress amplitude, usually normalized by initial vertical effective stress and expressed in the form of a cyclic stress ratio, CSR, for loading and a cyclic resistance ratio, CRR, for resistance. The potential for liquefaction is then described in terms of a factor of safety against liquefaction, $FS_L = CRR/CSR$.

Characterization of Earthquake Loading

The CSR is most commonly evaluated using the "simplified method" first described by Seed and Idriss (1971), which can be expressed as

$$CSR = 0.65\frac{a_{max}}{g} \cdot \frac{\sigma_{vo}}{\sigma'_{vo}} \cdot \frac{r_d}{MSF} \tag{1}$$

where a_{max}=peak ground surface acceleration; g=acceleration of gravity (in same units as a_{max}); σ_{vo}=initial vertical total stress; σ'_{vo}=initial vertical effective stress; r_d=depth reduction factor; and MSF=magnitude scaling factor, which is a function of earthquake magnitude. The depth reduction factor accounts for compliance of a typical soil profile, and the MSF acts as a proxy for the number of significant cycles, which is related to the ground

---

[1]Professor, Dept. of Civil and Environmental Engineering, Univ. of Washington, Seattle, WA 98195-2700. E-mail: kramer@u.washington.edu

[2]Consulting Engineer, Kirkland, WA 98034; formerly, Graduate Research Assistant, Dept. of Civil and Environmental Engineering, Univ. of Washington. E-mail: roy@mayfield.name

Note. Discussion open until December 1, 2007. Separate discussions must be submitted for individual papers. To extend the closing date by one month, a written request must be filed with the ASCE Managing Editor. The manuscript for this paper was submitted for review and possible publication on April 4, 2006; approved on July 20, 2006. This paper is part of the ***Journal of Geotechnical and Geoenvironmental Engineering***, Vol. 133, No. 7, July 1, 2007. ©ASCE, ISSN 1090-0241/2007/7-802–813/$25.00.

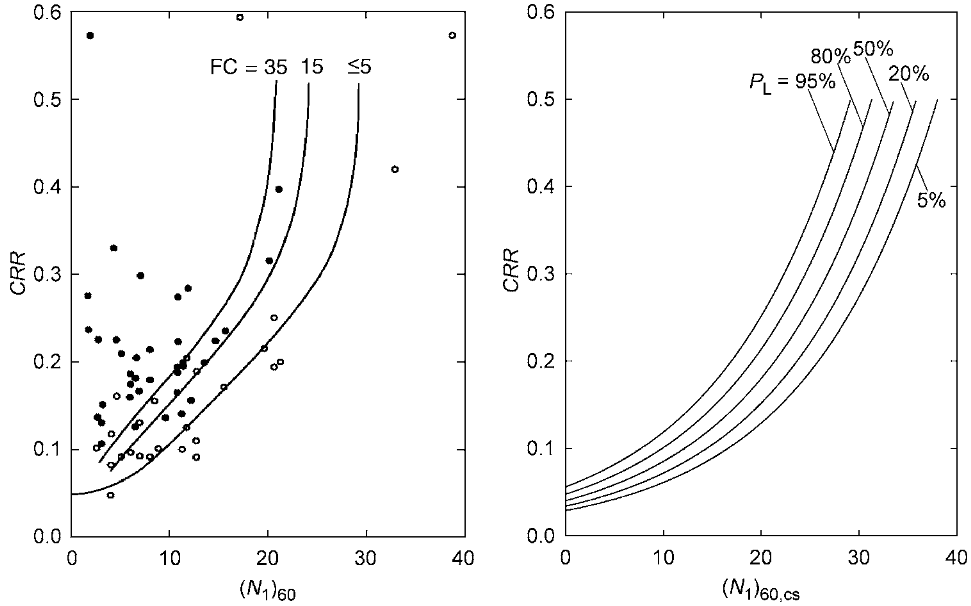

Fig. 1. (a) Deterministic cyclic resistance curves proposed by Youd et al. 2001, ASCE; (b) cyclic resistance curves of constant probability of liquefaction with measurement/estimation errors by Cetin et al. 2004, ASCE.

motion duration. It should be noted that two pieces of loading information—a_{max} and earthquake magnitude—are required for estimation of the CSR.

Characterization of Liquefaction Resistance

The CRR is generally obtained by correlation to in situ test results, usually standard penetration (SPT), cone penetration (CPT), or shear wave velocity (V_s) tests. Of these, the SPT has been most commonly used and will be used in the remainder of this paper. A number of SPT-based procedures for deterministic (Seed and Idriss 1971; Seed et al. 1985; Youd et al. 2001; Idriss and Boulanger 2004) and probabilistic (Liao et al. 1988; Toprak et al. 1999; Youd and Noble 1997; Juang and Jiang 2000; Cetin et al. 2004) estimation of liquefaction resistance have been proposed.

Deterministic Approach

Fig. 1(a) illustrates the widely used liquefaction resistance curves recommended by Youd et al. (2001), which are based on discussions at a National Center for Earthquake Engineering Research (NCEER) workshop (National Center for Earthquake Engineering Research 1997). The liquefaction evaluation procedure described by Youd et al. (2001) will be referred to hereafter as the NCEER procedure. The NCEER procedure has been shown to produce reasonable predictions of liquefaction potential (i.e., few cases of nonprediction for sites at which liquefaction was observed) in past earthquakes, and is widely used in contemporary geotechnical engineering practice. For the purposes of this paper, a conventionally liquefaction-resistant site will be considered to be one for which $FS_L \geqslant 1.2$ for a 475-year ground motion using the NCEER procedure. This standard is consistent with that recommended by Martin and Lew (1999), for example, and is considered representative of those commonly used in current practice.

Probabilistic Approach

Recently, a detailed review and careful reinterpretation of liquefaction case histories (Cetin 2000; Cetin et al. 2004) was used to develop new probabilistic procedures for the evaluation of liquefaction potential. The probabilistic implementation of the Cetin et al. (2004) procedure produces a probability of liquefaction, P_L, which can be expressed as

$$P_L = \Phi\left[-\frac{(N_1)_{60}(1+\theta_1\mathrm{FC}) - \theta_2 \ln \mathrm{CSR}_{\mathrm{eq}} - \theta_3 \ln M_w - \theta_4 \ln(\sigma'_{vo}/p_a) + \theta_5\mathrm{FC} + \theta_6}{\sigma_\varepsilon}\right] \quad (2)$$

where Φ=standard normal cumulative distribution function; $(N_1)_{60}$=corrected SPT resistance; FC=fines content (in percent); $\mathrm{CSR}_{\mathrm{eq}}$=cyclic stress ratio [Eq. (1) without MSF]; M_w=moment magnitude; σ'_{vo}=initial vertical effective stress, p_a is atmospheric pressure in same units as σ'_{vo}; σ_ε=measure of the estimated model and parameter uncertainty; and θ_1–θ_6 are model coefficients obtained by regression. As Eq. (2) shows, the probability of liquefaction includes both loading terms (again, peak acceleration, as reflected in the CSR, and magnitude) and resistance terms (SPT resistance, FC, and vertical effective stress). Mean values of the model coefficients are presented for two conditions in Table 1—a case in which the uncertainty includes parameter measurement/estimation errors and a case in which the effects of measurement/estimation errors have been removed. The former would corre-

Table 1. Cetin et al. (2004) Model Coefficients with and without Measurement/Estimation Errors (Adapted from Cetin et al. 2002)

Case	Measurement/estimation errors	θ_1	θ_2	θ_3	θ_4	θ_5	θ_6	σ_ε
I	Included	0.004	13.79	29.06	3.82	0.06	15.25	4.21
II	Removed	0.004	13.32	29.53	3.70	0.05	16.85	2.70

spond to uncertainties that exist for a site investigated with a normal level of detail and the latter to a "perfect" investigation [i.e., no uncertainty in any of the variables on the right-side of Eq. (2)]. Fig. 1(b) shows contours of equal P_L for conditions in which measurement/estimation errors are included; the measurement/estimation errors have only a slight influence on the model coefficients but a significant effect on the uncertainty term, σ_ε.

Direct comparison of the procedures described by Youd et al. (2001) and Cetin et al. (2004) is difficult because various aspects of the procedures are different. For example, Cetin et al. (2004) found that the average effective stress for their critical layers were at lower effective stresses ($\sim$0.65 atm) instead of the standard 1 atm, and made allowances for those differences. Also, the basic shapes of the cyclic resistance curves are different—the Cetin et al. (2004) curves (Fig. 3) have a smoothly changing curvature while the Youd et al. (2001) curve (Fig. 1) is nearly linear at intermediate SPT resistances $[(N_1)_{60} \approx 10-22]$ with higher curvatures at lower and higher SPT resistances. An approximate comparison of the two methods can be made by substituting CRR for $\mathrm{CSR}_{\mathrm{eq}}$ in Eq. (2) and then rearranging the equation in the form

$$\mathrm{CRR} = \exp\left[\frac{(N_1)_{60}(1+\theta_1\mathrm{FC}) - \theta_3 \ln M_w - \theta_4 \ln(\sigma'_{vo}/p_a) + \theta_5\mathrm{FC} + \theta_6 + \sigma_\varepsilon \Phi^{-1}(P_L)}{\theta_2}\right] \quad (3)$$

where Φ^{-1}=inverse standard normal cumulative distribution function. The resulting value of CRR can then be used in the common expression for FS_L. Arango et al. (2004) used this formulation without measurement/estimation errors (Case II in Table 1 and found that the Cetin et al. (2004) and NCEER procedures yielded similar values of FS_L for a site in San Francisco when a value of $P_L \approx 0.65$ was used in Eq. (3). A similar exercise for a site in Seattle with measurement/estimation errors (Case I in Table 1) shows equivalence of FS_L when a value of $P_L \approx 0.6$ is used. Cetin et al. (2004) suggest the use of a deterministic curve equivalent to that given by Eq. (3) with P_L=0.15, which would produce a more conservative result than the NCEER procedure. The differences between the two procedures are most pronounced at high CRR values; the NCEER procedure contains an implicit assumption of $(N_1)_{60}$=30 as an upper bound to liquefaction susceptibility while Cetin et al. (2004), whose database contained

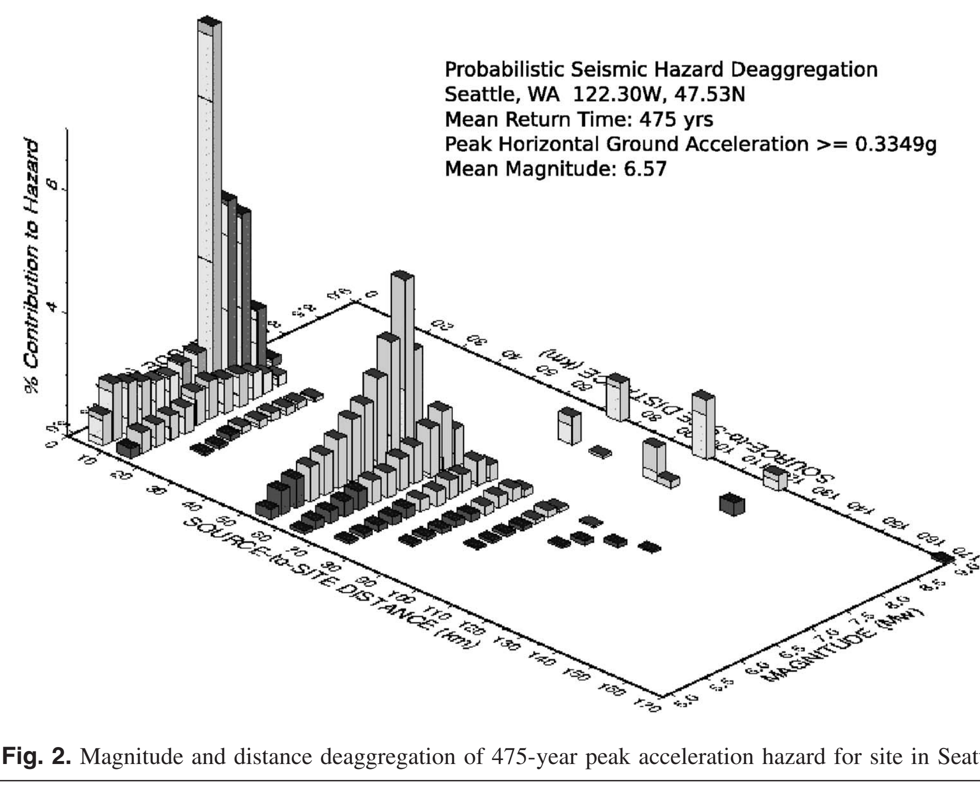

Fig. 2. Magnitude and distance deaggregation of 475-year peak acceleration hazard for site in Seattle

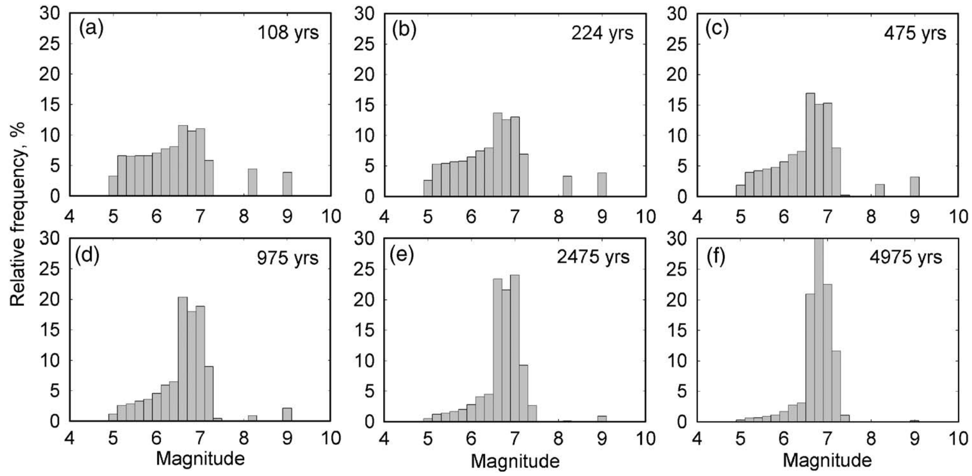

Fig. 3. Distributions of magnitude contributing to peak rock outcrop acceleration for different return periods in Seattle: (a) T_R=108 years; (b) T_R=224 years; (c) T_R=475 years; (d) T_R=975 years; (e) T_R=2,475 years; and (f) T_R=4,975 years

considerably more cases at high CSR levels, indicate that liquefaction is possible (albeit with limited potential effects) at $(N_1)_{60}$ values above 30.

Seismic Hazard Analysis

Ground shaking levels used in seismic design and hazard evaluations are generally determined by means of seismic hazard analyses. Deterministic seismic hazard analyses are used most often for special structures or for estimation of upper bound ground shaking levels. In the majority of cases, however, ground shaking levels are determined by probabilistic seismic hazard analyses.

Probabilistic seismic hazard analyses consider the potential levels of ground shaking from all combinations of magnitude and distance for all known sources capable of producing significant shaking at a site of interest. The distributions of magnitude and distance, and of ground shaking level conditional upon magnitude and distance, are combined in a way that allows estimation of the mean annual rate at which a particular level of ground shaking will be exceeded. The mean annual rate of exceeding a ground motion parameter value, y^*, is usually expressed as λ_{y^*}; the reciprocal of the mean annual rate of exceedance is commonly referred to as the return period. The results of a PSHA are typically presented in the form of a seismic hazard curve, which graphically illustrates the relationship between λ_{y^*} and y^*.

The ground motion level associated with a particular return period is therefore influenced by contributions from a number of different magnitudes, distances, and conditional exceedance probability levels (usually expressed in terms of a parameter, ε, defined as the number of standard deviations by which $\ln y^*$ exceeds the natural logarithm of the median value of y for a given M and R). The relative contributions of each M-R pair to λ_{y^*} can be quantified by means of a deaggregation analysis (McGuire, 1995); the deaggregated contributions of magnitude and distance are frequently illustrated in diagrams such as that shown in Fig. 2. Because both peak acceleration and magnitude are required for cyclic stress-based evaluations of liquefaction potential, the marginal distribution of magnitude can be obtained by summing the contributions of each distance and ε value for each magnitude; magnitude distributions for six return periods at a site in Seattle analyzed by the U.S. Geological Survey (USGS) (http://eqhazmaps.usgs.gov) are shown in Fig. 3. The decreasing significance of lower magnitude earthquakes for longer return periods, evident in Fig. 3, is a characteristic shared by many other locations.

Performance-Based Liquefaction Potential Evaluation

In practice, liquefaction potential is usually evaluated using deterministic CRR curves, a single ground motion hazard level, for example, for ground motions with a 475-year return period, and a single earthquake magnitude, usually the mean or mode. In contrast, the performance-based approach incorporates probabilistic CRR curves and contributions from *all* hazard levels and *all* earthquake magnitudes.

The roots of performance-based liquefaction assessment are in the method of seismic risk analysis introduced by Cornell (1968). The first known application of this approach to liquefaction assessment was presented by Yegian and Whitman (1978), although earthquake loading was described as a combination of earthquake magnitude and source-to-site distance rather than peak acceleration and magnitude. Atkinson et al. (1984) developed a procedure for the estimation of the annual probability of liquefaction using linearized approximations of the CRR curves of Seed and Idriss (1983) in a deterministic manner. Marrone et al. (2003) described liquefaction assessment methods that incorporate probabilistic CRR curves and the full range of magnitudes and peak accelerations in a manner similar to the PBEE framework described herein. Hwang et al. (2005) described a Monte Carlo simulation-based approach that produces similar results.

PBEE is generally formulated in a probabilistic framework to evaluate the risk associated with earthquake shaking at a particular site. The risk can be expressed in terms of economic loss, fatalities, or other measures. The Pacific Earthquake Engineering Research (PEER) has developed a probabilistic framework for PBEE (Cornell and Krawinkler 2000; Krawinkler 2002; Deierlein et al. 2003) that computes risk as a function of ground shaking through the use of several intermediate variables. The ground motion is characterized by an *intensity measure*, IM, which could be any one of a number of ground motion parameters (e.g., a_{max}, Arias intensity, etc.). The effects of the IM on a system of interest are expressed in terms used primarily by engineers in the form of *engineering demand parameters*, or EDPs (e.g., excess pore pressure, FS_L, etc.). The physical effects associated with the EDPs (e.g. settlement, lateral displacement, etc.) are expressed in terms of *damage measures*, or DMs. Finally, the risk associated with the DM is expressed in a form that is useful to decisionmakers by means of *decision variables*, DV (e.g. repair cost, downtime, etc.). The mean annual rate of exceedance of various DV levels, λ_{DV}, can be expressed in terms of the other variables as

$$\lambda_{dv} = \sum_{k=1}^{N_{DM}} \sum_{j=1}^{N_{EDP}} \sum_{i=1}^{N_{IM}} P[DV > dv | DM = dm_k] \times P[DM = dm_k | EDP = edp_j] P[EDP = edp_j | IM = im_i] \Delta\lambda_{im_i} \tag{4}$$

where $P[a|b]$ describes the conditional probability of a given b; and N_{DM}, N_{EDP}, and N_{IM} = number of increments of DM, EDP, and IM, respectively. Extending this approach to consider epistemic uncertainty in IM, although not pursued in this paper, is straightforward. By integrating over the entire hazard curve (approximated by the summation over $i=1$, N_{IM}), the performance-based approach includes contributions from all return periods, not just the return periods mandated by various codes or regulations.

For a liquefiable site, the geotechnical engineer's initial contribution to this process for evaluating liquefaction hazards comes primarily in the evaluation of $P[EDP|IM]$. Representing the EDP by FS_L and combining the probabilistic evaluation of FS_L with the results of a seismic hazard analysis allows the mean annual rate of *non*exceedance of a selected factor of safety, FS_L^*, to be computed as

$$\Lambda_{FS_L^*} = \sum_{i=1}^{N_{IM}} P[FS_L < FS_L^* | IM_i] \Delta\lambda_{IM_i} \tag{5}$$

The value of $\Lambda_{FS_L^*}$ should be interpreted as the mean annual rate (or inverse of the return period) at which the actual factor of safety will be less than FS_L^*. Note that $\Lambda_{FS_L^*}$ increases with increasing FS_L^* since weaker motions producing higher factors of safety occur more frequently than stronger motions that produce lower factors of safety. The mean annual rate of factor of safety nonexceedance is used because nonexceedance of a particular factor of safety represents an undesirable condition, just as exceedance of an intensity measure does; because lower case lambda is commonly used to represent mean annual rate of exceedance, an upper case lambda is used here to represent mean annual rate of nonexceedance. Since liquefaction is expected to occur when CRR < CSR (i.e., when $FS_L^* < 1.0$), the return period of liquefaction corresponds to the reciprocal of the mean annual rate of nonexceedance of $FS_L^* = 1.0$, i.e., $T_{R,L} = 1/\Lambda_{FS_L^*=1.0}$.

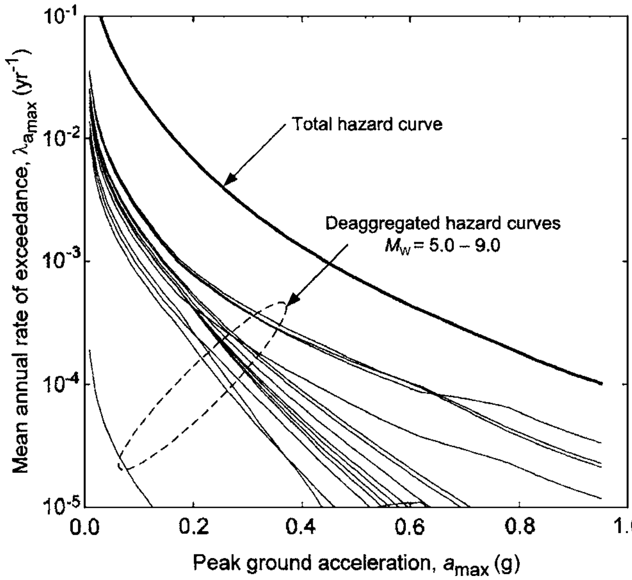

Fig. 4. Seismic hazard curves for Seattle deaggregated on the basis of magnitude. Total hazard curve is equal to sum of hazard curves for all magnitudes.

The PEER framework assumes IM sufficiency, i.e., that the intensity measure is a scalar that provides all of the information required to predict the EDP. This sufficiency, however, does not exist for cyclic stress-based liquefaction potential evaluation procedures as evidenced by the long-recognized need for a MSF. Therefore, FS_L depends on more than just peak acceleration as an intensity measure, and calculation of the mean annual rate of exceeding some factor of safety against liquefaction, FS_L^*, can be modified as

$$\Lambda_{FS_L^*} = \sum_{j=1}^{N_M} \sum_{i=1}^{N_{a_{max}}} P[FS_L < FS_L^* | a_{max_i}, m_j] \Delta\lambda_{a_{max_i}, m_j} \tag{6}$$

where N_M and $N_{a_{max}}$ = number of magnitude and peak acceleration increments into which "hazard space" is subdivided; and $\Delta\lambda_{a_{max_i}, m_j}$ = incremental mean annual rate of exceedance for intensity measure, a_{max_i}, and magnitude, m_j. The values of $\lambda_{a_{max}, m}$ can be visualized as a series of seismic hazard curves distributed with respect to magnitude according to the results of a deaggregation analysis (Fig. 3); therefore, their summation (over magnitude) yields the total seismic hazard curve for the site (Fig. 4). The conditional probability term in Eq. (6) can be calculated using the probabilistic model of Cetin et al. (2004), as described in Eq. (2), with $CSR = CSR_{eq,i} \cdot FS_L^*$ (with $CSR_{eq,i}$ computed from $a_{max,i}$) and $M_w = m_j$, i.e.

$$P[FS_L < FS_L^* | a_{max_i}, m_j] = \Phi\left[-\frac{(N_1)_{60}(1+\theta_1 FC) - \theta_2 \ln(CSR_{eq,i} \cdot FS_L^*) - \theta_3 \ln m_j - \theta_4 \ln(\sigma'_{vo}/p_a) + \theta_5 FC + \theta_6}{\sigma_\varepsilon} \right] \tag{7}$$

Another way of characterizing liquefaction potential is in terms of the liquefaction resistance required to produce a desired level of performance. For example, the SPT value required to resist liquefaction, N_{req}, can be determined at each depth of interest. The difference between the actual SPT resistance and the required SPT resistance would provide an indication of how much soil improvement might be required to bring a particular site to an acceptable factor of safety against liquefaction. Given that liquefaction would occur when $N < N_{req}$, or when $FS_L < 1.0$, then $P[N < N_{req}] = P[FS_L < 1.0]$. The PBEE approach can then be applied in such a way as to produce a mean annual rate of exceedance for N^*_{req}

$$\lambda_{N^*_{req}} = \sum_{j=1}^{N_M} \sum_{i=1}^{N_{a_{max}}} P[N_{req} > N^*_{req} | a_{max_i}, m_j] \Delta\lambda_{a_{max_i}, m_j} \tag{8}$$

where

$$P[N_{req} > N^*_{req} | a_{max_i}, m_j] = \Phi\left[-\frac{N^*_{req}(1 + \theta_1 FC) - \theta_2 \ln CSR_{eq,i} - \theta_3 \ln m_j - \theta_4 \ln(\sigma'_{vo}/p_a) + \theta_5 FC + \theta_6}{\sigma_\varepsilon} \right] \tag{9}$$

The value of N^*_{req} can be interpreted as the SPT resistance required to produce the desired performance level for shaking with a return period of $1/\lambda_{N^*_{req}}$.

Comparison of Conventional and Performance-Based Approaches

Conventional procedures provide a means for evaluating the liquefaction potential of a soil deposit for a given level of loading. When applied consistently to different sites in the same seismic environment, they provide a consistent indication of the likelihood of liquefaction (expressed in terms of FS_L or P_L) at those sites. The degree to which they provide a consistent indication of liquefaction likelihood when applied to sites in *different* seismic environments, however, has not been established. That issue is addressed in the remainder of this paper.

Idealized Site

Potentially liquefiable sites around the world have different likelihoods of liquefaction due to differences in site conditions (which strongly affect liquefaction resistance) and local seismic environments (which strongly affect loading). The effects of seismic environment can be isolated by considering the liquefaction potential of a single soil profile placed at different locations.

Fig. 5 shows the subsurface conditions for an idealized, hypothetical site with corrected SPT resistances that range from relatively low $[(N_1)_{60} = 10]$ to moderately high $[(N_1)_{60} = 30]$. Using the cyclic stress-based approach, the upper portion of the saturated sand would be expected to liquefy under moderately strong shaking. The wide range of smoothly increasing SPT resistance, while perhaps unlikely to be realized in a natural depositional environment, is useful for illustrating the main points of this paper.

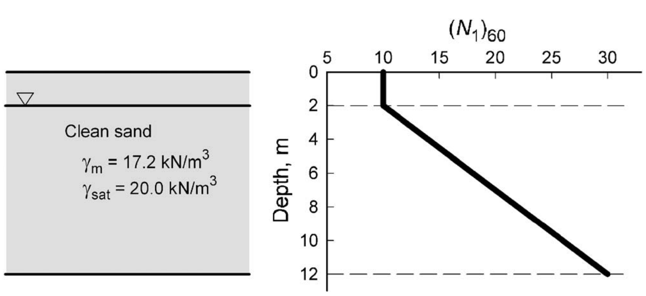

Fig. 5. Subsurface profile for idealized site

Locations

In order to illustrate the effects of different seismic environments on liquefaction potential, the hypothetical site was assumed to be located in each of the ten United States cities listed in Table 2. For each location, the local seismicity was characterized by the probabilistic seismic hazard analyses available from the USGS (using the 2002 interactive deaggregation link with listed latitudes and longitudes). In addition to being spread across the United States, these locations represent a wide range of seismic environments; the total seismic hazard curves for each of the locations are shown in Fig. 6. The seismicity levels vary widely—475-year peak acceleration values range from 0.12g (Butte) to 0.66g (Eureka). Two of the locations (Charleston and Memphis) are in areas of low recent seismicity with very large historical earthquakes, three (Seattle, Portland, and Eureka) are in areas subject to large-magnitude subduction earthquakes, and two (San Francisco and San Jose) are in close proximity (~60 km) in a very active environment.

Conventional Liquefaction Potential Analyses

Two sets of conventional deterministic analyses were performed to illustrate the different degrees of liquefaction potential of the

Table 2. Peak Ground Surface (Quaternary Alluvium) Acceleration Hazard Information for Ten U.S. Cities

Location	Latitude (N)	Longitude (W)	475-year a_{max}	2,475-year a_{max}
Butte, MT	46.003	112.533	0.120	0.225
Charleston, SC	32.776	79.931	0.189	0.734
Eureka, CA	40.802	124.162	0.658	1.023
Memphis, TN	35.149	90.048	0.214	0.655
Portland, OR	45.523	122.675	0.204	0.398
Salt Lake City, UT	40.755	111.898	0.298	0.679
San Francisco, CA	37.775	122.418	0.468	0.675
San Jose, CA	37.339	121.893	0.449	0.618
Santa Monica, CA	34.015	118.492	0.432	0.710
Seattle, WA	47.530	122.300	0.332	0.620

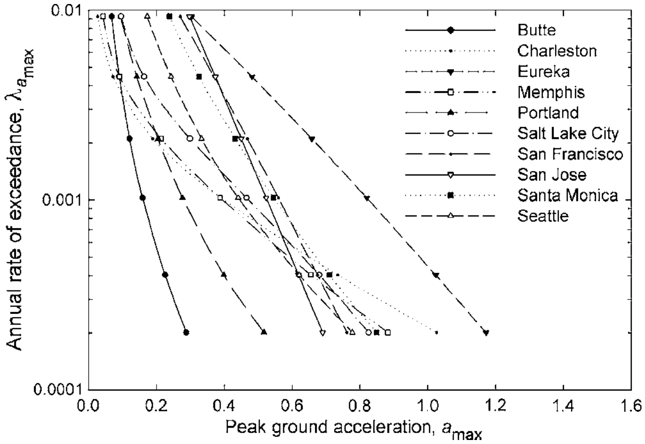

Fig. 6. USGS total seismic hazard curves for quaternary alluvium conditions at different site locations

hypothetical soil profile at the different site locations. The first set of analyses was performed using the NCEER procedure with 475-year peak ground accelerations and magnitude scaling factors computed using the mean magnitude from the 475-year deaggregation of peak ground acceleration. The second set of analyses was performed using Eq. (2) with $P_L=0.6$ to produce a deterministic approximation to the NCEER procedure; these analyses will be referred to hereafter as NCEER-C analyses. It should be noted that, although applied deterministically in this paper, the NCEER-C approximation to the NCEER procedure used here is *not* equivalent to the deterministic procedure recommended by Cetin et al. (2004). In all analyses, the peak ground surface accelerations were computed from the peak rock outcrop accelerations obtained from the USGS 2002 interactive deaggregations using a quaternary alluvium amplification factor (Stewart et al. 2003)

$$F_a = \frac{a_{\text{max,surface}}}{a_{\text{max,rock}}} = \exp[-0.15 - 0.13 \ln a_{\text{max,rock}}] \tag{10}$$

The amplification factor was applied deterministically so the uncertainty in peak ground surface acceleration is controlled by the uncertainties in the attenuation relationships used in the USGS PSHAs. The uncertainties in peak ground surface accelerations for soil sites are usually equal to or somewhat lower than those for rock sites (e.g., Toro et al. 1997; Stewart et al. 2003).

The results of the first set of analyses are shown in Fig. 7. Fig. 7(a) shows the variation of FS_L with depth for the hypothetical soil profile at each location. The results are, as expected, consistent with the seismic hazard curves—the locations with the highest 475-year a_{max} values have the lowest factors of safety against liquefaction. Fig. 7(b) expresses the results of the conventional analyses in a different way—in terms of $N_{\text{req}}^{\text{det}}$, the SPT resistance required to produce a performance level of $FS_L=1.2$ with the 475-year ground motion parameters for each location. The $(N_1)_{60}$ values for the hypothetical soil profile are also shown in Fig. 7(b), and can be seen to exceed the $N_{\text{req}}^{\text{det}}$ values at all locations/depths for which $FS_L > 1.2$. It should be noted that $N_{\text{req}}^{\text{det}} \leq 30$ for all cases since the NCEER procedure implies zero liquefaction potential (infinite FS_L) for $(N_1)_{60} > 30$.

The results of the second set of analyses are shown in Fig. 8, both in terms of FS_L and $N_{\text{req}}^{\text{det}}$. The FS_L and $N_{\text{req}}^{\text{det}}$ values are generally quite similar to those from the first set of analyses, except that required SPT resistances are slightly in excess of 30 (as allowed by the NCEER-C procedure) for the most seismically active locations in the second set. The similarity of these values confirms the approximation of the NCEER procedure by the NCEER-C procedure.

Performance-Based Liquefaction Potential Analyses

The performance-based approach, which allows consideration of all ground motion levels and fully probabilistic computation of liquefaction hazard curves, was applied to each of the site locations. Fig. 9 illustrates the results of the performance-based analy-

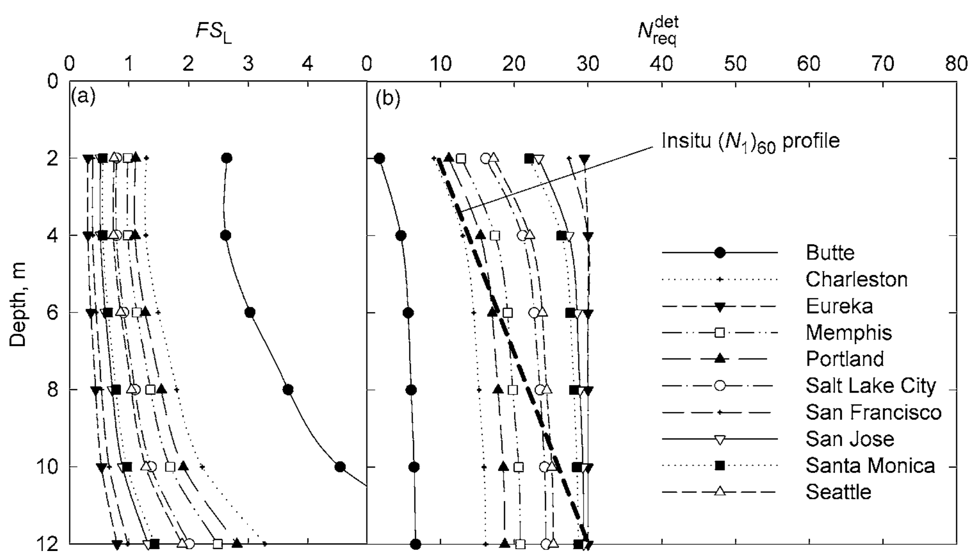

Fig. 7. Profiles of: (a) factor of safety against liquefaction; (b) required SPT resistance obtained using NCEER deterministic procedure with 475-year ground motions

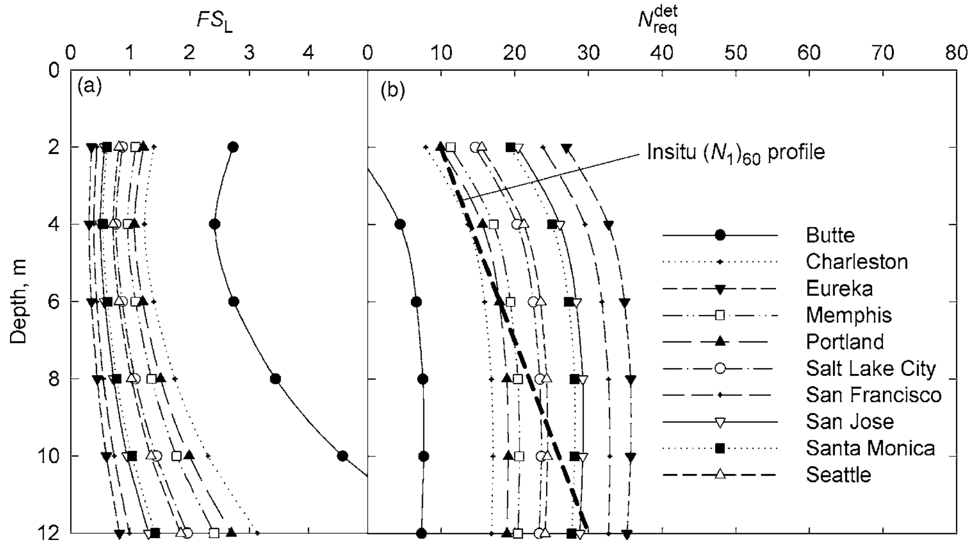

Fig. 8. Profiles of: (a) factor of safety against liquefaction; (b) required SPT resistance obtained using NCEER-C deterministic procedure for 475-year ground motions

ses for an element of soil near the center of the saturated zone (at a depth of 6 m, at which $(N_1)_{60}=18$ for the hypothetical soil profile). Fig. 9(a) shows factor of safety hazard curves, and Fig. 9(b) shows hazard curves for $N_{\text{req}}^{\text{PB}}$, the SPT resistance required to resist liquefaction. Note that the SPT resistances shown in Fig. 9(b) are those at which liquefaction would actually be expected to occur, rather than the values at which FS_L would be as low as 1.2 (corresponding to a conventionally liquefaction resistant soil as defined previously), which were plotted in Figs. 7 and 8. Therefore, the mean annual rates of exceedance in Fig. 9 are equal at each site location for $\text{FS}_L=1.0$ and $N_{\text{req}}^{\text{PB}}=18$.

Equivalent Return Periods

The results of the conventional deterministic analyses shown in Figs. 7 and 8 can be combined with the results of the performance-based analyses shown in Fig. 9 to evaluate the return periods of liquefaction produced in different areas by consistent application of conventional procedures for evaluation of liquefaction potential. For each site location, the process is as follows:

1. At the depth of interest, determine the SPT resistance required to produce a factor of safety of 1.2 using the conventional approach [from either Figs. 7(b) or 8(b)]. At that SPT resistance, the soils at that depth would have an equal liquefaction potential (i.e., $\text{FS}_L=1.2$ with a 475-year ground motion) at all site locations as evaluated using the conventional approach.
2. Determine the mean annual rate of exceedance for the SPT resistance from Step 1 using results of the type shown in Fig. 9(b) for each depth of interest. Since Fig. 9(b) shows the SPT resistance for $\text{FS}_L=1.0$, this is the mean annual rate of liquefaction for soils with this SPT resistance at the depth of interest.
3. Compute the return period as the reciprocal of the mean annual rate of exceedance.

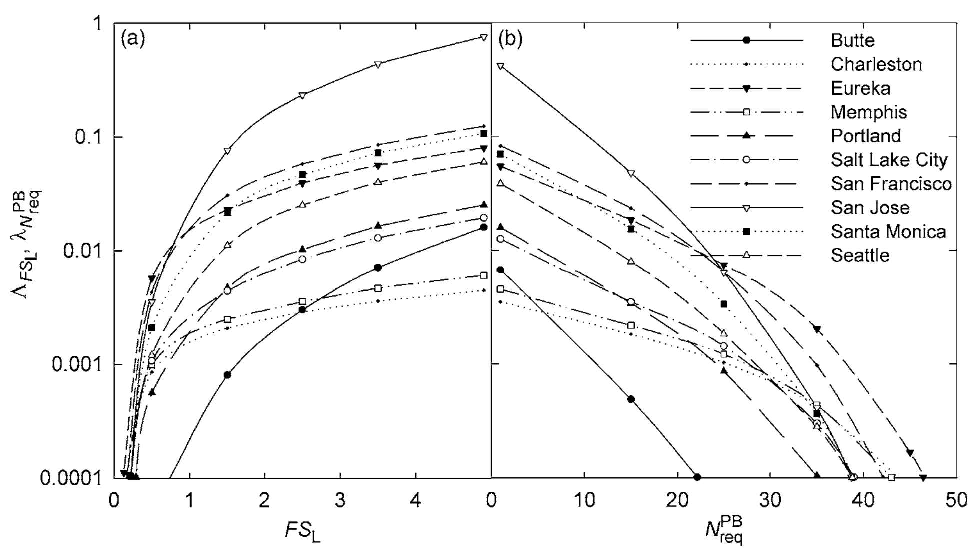

Fig. 9. Seismic hazard curves for 6-m depth: (a) factor of safety against liquefaction, FS_L for $(N_1)_{60}=18$; (b) required SPT resistance, $N_{\text{req}}^{\text{PB}}$, for $\text{FS}_L=1.0$

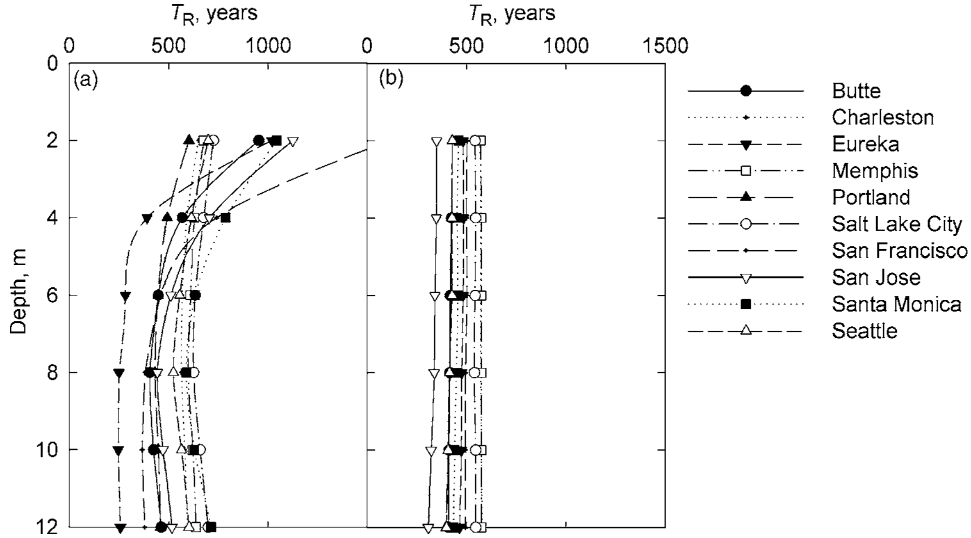

Fig. 10. Profiles of return period of liquefaction for sites with equal liquefaction potential as evaluated by (a) NCEER procedure; (b) NCEER-C procedure using 475-year ground motion parameters

4. Repeat Steps 1–3 for each depth of interest.

This process was applied to all site locations in Table 2 to evaluate the return period for liquefaction as a function of depth for each location; the calculations were performed using 475-year ground motions and again using 2,475-year ground motions.

Fig. 10 shows the results of this process for both sets of conventional analyses. It is obvious from Fig. 10 that consistent application of the conventional procedure produces inconsistent return periods, and therefore different actual likelihoods of liquefaction, at the different site locations. Examination of the return period curves shows that they are nearly vertical at depths greater than about 4 m, indicating that the deterministic procedures are relatively unbiased with respect to SPT resistance. The greater verticality of the curves based on the NCEER-C analyses results from the consistency of the shapes of those curves and the constant P_L curves given by Eq. (2), which were used in the performance-based analyses. Differences between the shapes of the NCEER curve [Fig. 1(a)] and the curves [Fig. 1(b)], particularly for sites subjected to very strong shaking (hence, very high CSRs) such as San Francisco and Eureka, contribute to depth-dependent return periods for the NCEER results.

Table 3. Liquefaction Return Periods for 6 m Depth in Idealized Site at Different Site Locations Based on Conventional Liquefaction Potential Evaluation Using 475-year and 2,475-year Motions

	475-year motions		2,475-year motions	
Location	NCEER	NCEER-C	NCEER	NCEER-C
Butte, MT	348	418	1,592	2,304
Charleston, SC	532	571	1,433[a]	2,725
Eureka, CA	236[a]	483	236[a]	1,590
Memphis, TN	565	575	1,277[a]	2,532
Portland, OR	376	422	1,675	1,508
Salt Lake City, UT	552	543	1,316[a]	2,674
San Francisco, CA	355[a]	503	355[a]	1,736
San Jose, CA	360	341	532[a]	1,021
Santa Monica, CA	483	457	794[a]	1,901
Seattle, WA	448	427	1,280[a]	2,155

[a]Upper limit of $(N_1)_{60}=30$ implied by NCEER procedure reached.

Table 3 shows the return periods of liquefaction at a depth of 6 m (the values are approximately equal to the averages over the depth of the saturated zone for each site location) for conditions that would be judged as having equal liquefaction potential using conventional procedures. Using both the NCEER and NCEER-C procedures, the actual return periods of liquefaction can be seen to vary significantly from one location to another, particularly for the case in which the conventional procedure was used with 2,475-year motions.

The actual return periods depend on the seismic hazard curves and deaggregated magnitude distributions, and are different for the NCEER and NCEER-C procedures. Using the NCEER procedure with 475-year motions, the actual return periods of liquefaction range from as short as 236 years [for Eureka, which is affected by the $(N_1)_{60}=30$ limit implied by the NCEER procedure] to 565 years (Memphis); the corresponding 50-year probability of liquefaction (under the Poisson assumption) in Eureka would be more than double that in Memphis. The return periods computed using the NCEER-C procedure with 475-year motions are more consistent, but still range from 341 years (San Jose) to about 570 years (Charleston and Memphis).

If deterministic liquefaction potential evaluations are based on 2,475-year ground motions using the NCEER procedure, the implied limit of $(N_1)_{60}=30$ produces highly inconsistent actual return periods—the 50-year probability of liquefaction in Eureka would be more than six times that in Portland. All but two of the ten locations would require $(N_1)_{30}=30$ according to that procedure and, as illustrated in Fig. 9(b), the return periods for $N_{req}^{PB}=30$ vary widely in the different seismic environments. The variations are smaller but still quite significant using the NCEER-C procedure.

Differences in regional seismicity can produce significant differences in ground motions at different return periods. Leyendecker et al. (2000) showed that short-period (0.2 s) spectral acceleration, for example, increased by about 50% when going from return periods of 475 years to 2,475 years in Los Angeles and San Francisco but by 200–500% or more in other areas of the country. The position and slope of the peak acceleration hazard curve clearly affect the return period of liquefaction. However, the regional differences in magnitude distribution (i.e., the rela-

Table 4. Required Penetration Resistances for 475-year Liquefaction Hazard in Element of Soil at 6 m Depth in Hypothetical Site at Different Site Locations, and Ratios of Equivalent Factors of Safety

Location	NCEER N_{req}^{det}	NCEER-C N_{req}^{det}	475-year N_{req}^{PB}	NCEER $\frac{CRR(N_{req}^{det})}{CRR(N_{req}^{PB})}$	NCEER-C $\frac{CRR(N_{req}^{det})}{CRR(N_{req}^{PB})}$
Butte, MT	5.6	6.6	7.3	0.88	0.95
Charleston, SC	14.5	15.9	12.1	1.19	1.32
Eureka, CA	30.0	34.9	34.8	0.0[a]	1.01
Memphis, TN	19.1	19.4	15.7	1.28	1.31
Portland, OR	17.0	17.9	18.8	0.88	0.94
Salt Lake City, UT	22.7	22.5	21.1	1.12	1.11
San Francisco, CA	30.0	31.8	31.5	0.0[a]	1.02
San Jose, CA	28.5	28.3	29.6	0.92	0.91
Santa Monica, CA	27.6	27.3	27.5	1.01	0.99
Seattle, WA	23.8	23.5	24.2	0.97	0.95

[a]Zero values caused by upper limit of $(N_1)_{60}=30$ implied by NCEER procedure.

tive contribution to peak acceleration hazard from each magnitude) also contribute to differences in return period; San Francisco and San Jose have substantially different return periods for liquefaction despite the similarity of their hazard curves because the relative contributions of large magnitude earthquakes on the San Andreas fault are higher for San Francisco than for San Jose.

Conditions for Consistent Liquefaction Potential

The differences in actual liquefaction return periods produced by conventional liquefaction potential evaluations make it difficult to establish uniform and consistent procedures for conventional evaluation of seismic hazards such as liquefaction potential. The performance-based approach, however, provides a framework in which design and evaluation can be based on a specified return period for liquefaction rather than on the basis of a factor of safety or probability of liquefaction for a ground motion with a specified return period. It is useful to compare the differences in possible requirements for acceptable liquefaction resistance produced by the conventional and performance-based approaches. For the purposes of this paper, two alternative criteria will be considered:

1. The previously described conventional criterion of a minimum $FS_L=1.2$ with 475-year ground motions; and
2. A performance-based criterion of a 475-year return period for liquefaction, i.e., $T_R(FS_L=1.0)=475$ years.

The 475-year return period used in the second criterion is intended as an example; a suitable specific return period for an actual performance-based liquefaction criterion would need to be identified and endorsed by a group of experienced professionals.

The SPT resistances required to satisfy the first criterion at a depth of 6 m, computed using the NCEER and NCEER-C procedures, are listed in Table 4, as well as the SPT resistances required to satisfy the second criterion at the same depth. For those locations at which the return periods for liquefaction in Table 3 were less than 475 years, the SPT resistances required for liquefaction with an actual return period of 475 years are increased, and vice versa for locations at which the Table 2 return periods were greater than 475 years. For a location like Memphis, the relative conservatism in the conventional approach means that the required SPT resistance of 19.1 for $FS_L=1.2$ with the 475-year motion (NCEER procedure) is reduced to an SPT resistance of 14.3 for a 475-year return period of liquefaction (performance-based procedure). For Portland, the relative unconservatism in the conventional approach means that the required SPT resistance increases slightly from 17.0 (deterministic procedure) to 17.5 (performance-based procedure).

Because cyclic resistance ratio varies nonlinearly with SPT resistance, it is also useful to consider the difference between the deterministic and performance-based approaches from a factor of safety standpoint. Since FS_L is proportional to CRR, the ratio of the CRR values corresponding to the SPT resistances in Table 4 can be thought of as factor of safety ratios that describe the "extra" liquefaction resistance required by the deterministic criterion ($FS_L=1.2$ for 475-year ground motion) relative to that required by the performance-based criterion (475-year return period for liquefaction). These values, shown in Table 4, range from 0.88 to 1.28 for the NCEER procedure and from 0.91 to 1.32 for the NCEER-C procedure; higher values are associated with locations that are "penalized" by conventional deterministic procedures. The zero values shown for Eureka and San Francisco result from the fact that $N_{req}^{PB}>30$ for those highly active areas; the corresponding CRR from the NCEER procedure is infinite. In Memphis and Charleston, for example, the deterministic criterion would result in a factor of safety some 30% higher than that associated with an actual return period of 475 years. At several other locations, the same deterministic criterion would result in factors of safety *lower* than those associated with the same actual liquefaction hazard. In effect, the conventional procedure results in an owner in Memphis designing for an equivalent factor of safety that is about 45% higher than an owner in Portland.

Summary and Conclusions

The evaluation of liquefaction potential involves comparison of consistent measures of loading and resistance. In contemporary geotechnical engineering practice, such comparisons are commonly made using cyclic shear stresses expressed in terms of normalized cyclic stress and cyclic resistance ratios. The CSR is usually estimated using a simplified procedure in which the level of ground shaking is related to peak ground surface acceleration and earthquake magnitude. Criteria by which liquefaction resistance is judged to be adequate are usually expressed in terms of a single level of ground shaking.

For a given soil profile at a given location, liquefaction can be caused by a range of ground shaking levels—from strong ground motions that occur relatively rarely to weaker motions that occur more frequently. Performance-based procedures allow consideration of all levels of ground motion in the evaluation of liquefaction potential. By integrating a probabilistic liquefaction evaluation procedure with the results of a PSHA, this paper presented a methodology for performance-based evaluation of liquefaction potential. The methodology was used to illustrate differences between performance-based and conventional evaluation of liquefaction potential. These analyses led to the following conclusions:

1. The actual potential for liquefaction, considering all levels of ground motion, is influenced by the position and slope of the peak acceleration hazard curve and by the distributions of earthquake magnitude that contribute to peak acceleration hazard at different return periods.
2. Consistent application of conventional procedures for evaluation of liquefaction potential (i.e., based on a single ground motion level) to sites in different seismic environments can produce highly inconsistent estimates of actual liquefaction hazards.
3. Criteria based on conventional procedures for evaluation of liquefaction potential can produce significantly different liquefaction hazards even for sites in relatively close proximity to each other. For the locations considered in this paper, such criteria were generally more strict (i.e., resulted in longer return periods, hence lower probabilities, of liquefaction) for locations with flatter peak acceleration hazard curves than for locations with steeper hazard curves, and for locations at which large magnitude earthquakes contributed a relatively large proportion of the total hazard.
4. Criteria that would produce more uniform liquefaction hazards at locations in all seismic environments could be developed by specifying a standard return period for liquefaction. Performance-based procedures such as the one described in this paper could be used to evaluate individual sites with respect to such criteria.

The performance-based methodology described in this paper makes use of a recently developed procedure for estimation of the probability of liquefaction. While this procedure is very well suited for implementation into the performance-based methodology, other probabilistic liquefaction procedures could also be used. The methodology, which deals with the initiation of liquefaction, can also be extended to estimate return periods for various effects of liquefaction such as lateral spreading displacement or ground surface settlement; research on these issues is underway.

Acknowledgments

The research described in this paper was funded by the Washington State Department of Transportation; the support of Tony Allen and Kim Willoughby is gratefully acknowledged. A portion of the work was completed while the senior writer was on sabbatical leave at the International Centre for Geohazards at the Norwegian Geotechnical Institute, where he benefited greatly from discussions with Dr. Farrokh Nadim. The performance-based approach described in the paper was motivated by the senior writer's involvement with PEER, and particularly by discussions with Professor C. Allin Cornell. The writers are grateful to Dr. Donald G. Anderson, Professor Stephen E. Dickenson, Dr. Robert M. Pyke, Professor Jonathan P. Stewart, and Steven G. Vick for their constructive comments.

References

Arango, I., Ostadan, F., Cameron, J., Wu, C. L., and Chang, C. Y. (2004). "Liquefaction probability of the BART Transbay Tube backfill." *Proc., 11th Int. Conf. on Soil Dynamics and Earthquake Engineering and 3rd Int. Conf. on Earthquake Geotechnical Engineering*, Berkeley, Calif., I, 456–462.

Atkinson, G. M., Finn, W. D. L., and Charlwood, R. G. (1984). "Simple computation of liquefaction probability for seismic hazard applications." *Earthquake Spectra*, 1(1), 107–123.

Cetin, K. O. (2000). "Reliability-based assessment of seismic soil liquefaction initiation hazard." Ph.D. dissertation, Univ. of California, Berkeley.

Cetin, K. O., et al. (2004). "Standard penetration test-based probabilistic and deterministic assessment of seismic soil liquefaction potential." *J. Geotech. Geoenviron. Eng.*, 130(12), 1314–1340.

Cetin, K. O., Der Kiureghian, A., and Seed, R. B. (2002). "Probabilistic models for the initiation of soil liquefaction." *Struct. Safety* 24, 67–82.

Cornell, C. A. (1968). "Engineering seismic risk analysis." *Bull. Seismol. Soc. Am.* 58(5), 1583–1606.

Cornell, C. A., and Krawinkler, H. (2000). "Progress and challenges in seismic performance assessment." *PEER News*, April 1–3, PEER, Berkeley, Calif.

Deierlein, G. G., Krawinkler, H., and Cornell, C. A. (2003). "A framework for performance-based earthquake engineering." *Proc., 2003 Pacific Conf. on Earthquake Engineering*, Wellington, New Zealand.

Idriss, I. M., and Boulanger, R. W. (2004). "Semiempirical procedures for evaluating liquefaction potential during earthquakes." *Proc., 11th Int. Conf. on Soil Dynamics and Earthquake Engineering and 3rd Int. Conf. on Earthquake Geotechnical Engineering*, Berkeley, Calif., I, 32–56.

Hwang, J. H., Chen, C. H., and Juang, C. H. (2005). "Liquefaction hazard analysis: A fully probabilistic method." *Proc., of the Sessions of the Geo-Frontiers 2005 Congress*, Earthquake Engineering and Soil Dynamics, R. W. Boulanger et al., eds, ASCE, Reston, Va., Paper No. 22.

Juang, C. H., and Jiang, T. (2000). "Assessing probabilistic methods for liquefaction potential evaluation." *Soil dynamics and liquefaction 2000*, R. Y. S. Pak and J. Yamamuro, eds., Geotechnical Special Publication, 107, ASCE, New York, 148–162.

Krawinkler, H. (2002). "A general approach to seismic performance assessment." *Proc., Int. Conf. on Advances and New Challenges in Earthquake Engineering Research*, ICANCEER, Hong Kong.

Leyendecker, E. V., Hunt, R. J., Frankel, A. D., and Rukstales, K. R. (2000). "Development of maximum considered earthquake ground motion maps." *Earthquake Spectra*, 16(1), 21–40.

Liao, S. S. C., Veneziano, D., and Whitman, R. V. (1988). "Regression models for evaluating liquefaction probability." *J. Geotech. Engrg.*, 114(4), 389–411.

Marrone, J., Ostadan, F., Youngs, R., and Litehiser, J. (2003). "Probabilistic liquefaction hazard evaluation: Method and application." *Proc., 17th Int. Conf. Structural Mechanics in Reactor Technology (SMiRT 17)*, Prague, Czech Republic, Paper No. M02-1.

Martin, G. R., and Lew, M., eds. (1999). "Recommended procedures for implementation of DMG Special Publication 117—Guidelines for analyzing and mitigating liquefaction hazards in California." Southern California Earthquake Center, Los Angeles.

McGuire, R. K. (1995). "Probabilistic seismic hazard analysis and design earthquakes: Closing the loop." *Bull. Seismol. Soc. Am.*, 85(5), 1275–1284.

National Center for Earthquake Engineering Research. (1997). *Proc., NCEER Workshop on Evaluation of Liquefaction Resistance of Soils*, T. L. Youd and I. M. Idriss eds., *Technical Rep. No. NCEER, 97-022*, NCEER, Buffalo, N.Y.

Seed, H. B., and Idriss, I. M. (1971). "Simplified procedure for evaluating soil liquefaction potential." *J. Soil Mech. and Found. Div.* 97, 1249–1273.

Seed, H. B and Idriss, I. M (1983). *Ground motions and soil liquefaction during earthquakes*, Earthquake Engineering Research Institute, Berkeley, Calif., 134.

Seed, H. B., Tokimatsu, K., Harder, L. F., and Chung, R. M. (1985). "Influence of SPT procedures in soil liquefaction resistance evaluations." *J. Geotech. Engrg.*, 111(12), 1425–1445.

Stewart, J. P., Liu, A. H., and Choi, Y. (2003). "Amplification factors for spectral acceleration in tectonically active regions." *Bull. Seismol. Soc. Am.*, 93(1), 332–352.

Toprak, S., Holzer, T. L., Bennett, M. J., and Tinsley, J. C. III. (1999). "CPT- and SPT-based probabilistic assessment of liquefaction." *Proc., 7th U.S.-Japan Workshop on Earthquake Resistant Design of Lifeline Facilities and Countermeasures Against Liquefaction*, Multidisciplinary Center for Earthquake Engineering Research, Buffalo, N.Y., 69–86.

Toro, G. R., Abrahamson, N. A., and Schneider, J. F. (1997). "Model of strong ground motions from earthquakes in central and eastern North America: Best estimates and uncertainties." *Seismol. Res. Lett.*, 68(1), 41–57.

Yegian, M. Y., and Whitman, R. V. (1978). "Risk analysis for ground failure by liquefaction." *J. Geotech. Engrg. Div.*, 104, 921–938.

Youd, T. L., et al. (2001). "Liquefaction resistance of soils: Summary report from the 1996 NCEER and 1998 NCEER/NSF workshops on evaluation of liquefaction resistance of soils." *J. Geotech. Geoenviron. Eng.*, 127, 817–833.

Youd, T. L., and Noble, S. K. (1997). "Liquefaction criteria based on statistical and probabilistic analyses." *Proc., NCEER Workshop on Evaluation of Liquefaction Resistance of Soils*, National Center for Earthquake Engineering Research, Buffalo, N.Y., 201–205.